Interplay of model ingredients affecting aggregate shape plasticity in diffusion-limited aggregation

P. Duarte-Neto,[1,2] T. Stošić,[1] B. Stošić,[1] R. Lessa,[3] and M. V. Milošević[2,4,*]

[1]*Departamento de Estatística e Informática, Universidade Federal Rural de Pernambuco, 52171-900 Recife, Brazil*

[2]*Departement Fysica, Universiteit Antwerpen, Groenenborgerlaan 171, B-2020 Antwerpen, Belgium*

[3]*Departamento de Pesca e Aquicultura, Universidade Federal Rural de Pernambuco, 52171-900 Recife, Brazil*

[4]*Departamento de Física, Universidade Federal do Ceará, Caixa Postal 6030, Campus do Pici, 60455-900 Fortaleza, Ceará, Brazil*

(Received 11 September 2013; revised manuscript received 17 May 2014; published 31 July 2014)

We analyze the combined effect of three ingredients of an aggregation model—surface tension, particle flow and particle source—representing typical characteristics of many aggregation growth processes in nature. Through extensive numerical experiments and for different underlying lattice structures we demonstrate that the location of incoming particles and their preferential direction of flow can significantly affect the resulting general shape of the aggregate, while the surface tension controls the surface roughness. Combining all three ingredients increases the aggregate shape plasticity, yielding a wider spectrum of shapes as compared to earlier works that analyzed these ingredients separately. Our results indicate that the considered combination of effects is fundamental for modeling the polymorphic growth of a wide variety of structures in confined geometries and/or in the presence of external fields, such as rocks, crystals, corals, and biominerals.

DOI: 10.1103/PhysRevE.90.012312 PACS number(s): 61.43.Hv, 47.57.eb, 68.35.B−

I. INTRODUCTION

Simulation growth models are readily used to describe a wide range of natural structures [1]. They are usually devised to reflect the essential features of a specific growth phenomenon, but often remain applicable to many other natural phenomena. The choice of the most appropriate model to explain the growth observed in a given system is based on identification of the minimal set of factors that govern formation of large structures by aggregation of small subunits (particles) and lead to a realistic description of the phenomenon in question. In order to make this choice, the relevance of each possible ingredient factor should be examined separately and the effect of combining these factors should be fully understood.

A wide variety of materials and biological structures are formed by aggregation [2], a process where identical particles are joined into clusters according to some general rule. Numerical experiments devised to simulate these phenomena are usually carried out on regular lattices, where the diameter of the particles is taken to correspond to the lattice spacing and the characteristics of the trajectory of the incoming particles play a decisive role in the resultant formation and shape of the aggregate [1–3]. However, in order to better understand a variety of shapes of physical, chemical, and biological species-specific structures (e.g., fish otoliths [4] and stony corals [5]), further studies are needed to distinguish between the effects of various individual microscopic model ingredients, and their combined effects, on the shape of the aggregated structure.

Diffusion-limited aggregation (DLA), introduced by Witten and Sander in 1981 [6], is one of the most commonly used models to simulate the growth by aggregation of natural structures, including biological phenomena such as bacterial, neural, and stony coral growth [2,5,7]. Due to the simplicity of its algorithm and the realism of the resulting aggregates, this model plays a paradigmatic role in the field of kinetic growth phenomena [8]. The standard DLA is based on the following process. A seed particle is fixed at a central point of the substrate and another particle is released from a random position of a circle far away from the seed. The released particle moves according to a Brownian trajectory until it reaches one of the sites on the perimeter of the seed, where it is fixed, forming a cluster of two particles. This process is carried out repeatedly by releasing particles from the far away perimeter until they reach the existing cluster and stick to it.

Several generalizations of the original DLA model have been proposed, by considering, e.g., changes in particle density [9,10], surface tension [11,12], or particle flow (drift) [13–15]. In particular, changes in surface tension lead to more compact aggregates [11,12,16], while modification of particle flux produces anisotropic ramified clusters that grow in the flux direction [13–15]. While these generalizations are certainly justified for simulations of various natural processes and are thus plausible ingredients of a microscopic growth model for many natural phenomena, they have been treated separately in the past, therefore producing a rather narrow range of shapes.

In the present work we show that the combination and in some cases competing effects of these model ingredients can provide a much wider range of resulting aggregate shapes. To further widen the spectrum of natural growth phenomena that may be emulated, we additionally simulate a localized source of particles (as is frequently the case in nature) rather than launching particles uniformly from a distant perimeter. Moreover, the effects of these ingredients were evaluated for different underlying lattice structure for aggregation, as well as different properties of the confinement and the boundary condition. Finally, we show how the morphology of obtained shapes can be analyzed, classified, and compared to self-assembled systems in nature using their basic geometric properties.

The paper is organized as follows. In Sec. II we describe the simulation framework. The results are shown first for varied surface tension (sticking probability) in Sec. III and then expanded by analysis of the additional influence of particle flow and location of the particle source in Secs. IV and V,

*Corresponding author: milorad.milosevic@uantwerpen.be

 ©2014 American Physical Society

respectively. Finally, in Sec. VI we reveal the relevance of our results to the morphology of various objects in nature, particularly ones formed by biomineralization, and show how the obtained shapes can be compared and their differences quantified so that model can be further improved. Our findings are summarized in Sec. VII.

II. NUMERICAL SIMULATIONS

In this paper we examine the effects of additional model ingredients to the generalized DLA model proposed by Batchelor and Henry [12], which takes into account the local sticking probability of the constituent particles in aggregation. For aggregation on a square lattice, the sticking probability is defined as

$$s = \alpha_p^{3-B}, \tag{1}$$

where $0 < \alpha_p < 1$ is a parameter corresponding to local surface tension and $B \in \{1,2,3\}$ is the number of neighboring sites experienced by the incoming particle.

However, DLA on a square lattice is known to suffer from pronounced anisotropy of the aggregates. As reported by Meakin [17], lower anisotropy is obtained by growing clusters on an off-lattice DLA or on lattices with fivefold or higher symmetry. In the current work we address several modifications of the original algorithm, with the intent of enhancing the realism of the numerical simulations. First, one can modify the restriction in the number of possible directions for the random walk. For instance, for a triangular lattice the particle moves randomly in six directions or one can use a continuous random walk instead of a walk on a lattice (i.e., off-lattice DLA). Another modification concerns the growing directions, i.e., change in the number of neighboring sites experienced by the incoming particles. Namely, in the DLA of Batchelor and Henry the definition of the number of nearest neighbors and the corresponding sticking probabilities (on the underlying lattice) has a crucial role. In Ref. [16], DLA generalization was extended to a triangular lattice, where the sticking probability s was introduced as

$$s = \alpha_p^{5-B} \tag{2}$$

for $B \in \{1,\ldots,5\}$ first neighbors. However, the number of neighbors cannot be universally defined for the off-lattice model, i.e., it depends on particular system to be simulated, where the definition of sticking probability should reflect the underlying (particular) crystal structure, or the properties of the underlying protein network (as in the case of calcified organs in living organisms). We therefore adopt in the current paper the most general pragmatic approach: For off-lattice DLA we perform a continuous random walk of particles, but we apply the sticking algorithm using blocks (or pixels) on a square lattice grid. As soon as the given block (pixel) is occupied by a particle, the block (pixel) is labeled as occupied, the coordinate of the occupying particle is discarded, and thereon the sticking probability of new incoming particles is defined in relation to the existing occupied block structure [either the four nearest neighbors, using Eq. (1), or all eight immediate neighbors on a square lattice, where $s = \alpha_p^{7-B}$ and $B \in \{1,\ldots,7\}$].

Indeed, the DLA algorithm can be relatively easily generalized and numerous scenarios can be investigated, depending on the system to be studied. For the purpose of this paper, we concentrate efforts on the simplest possible approach that captures relevant physics, i.e., DLA on a square lattice, and perform a detailed analysis of several important ingredients in the model. Nevertheless, we also show results for other above-described modifications in order to present an extensive discussion of the role of all growth conditions on the obtained agglomerates.

In particular, the DLA model is studied under external factors and in the presence of certain confinement, where in addition to the local sticking probability the eventual directional bias in movement and the nonuniform distribution of launched particles are also taken into account. More precisely, three distinct scenarios are considered.

(1) In the generalized DLA model of Batchelor and Henry [12] in circular confinement, the surface tension α_p is varied.

(2) For each α_p value, the probabilities of motion of particles in different directions are modified so that, e.g., probability ρ_1 for motion in one direction is increased (simulating flow), while the motion in the other three directions is taken to be equiprobable $[(1-\rho_1)/3]$. We also consider the case of more probable motion in two directions on a square lattice, as well as the off-lattice spatial distribution of motion probabilities favoring a particular direction of flow.

(3) Instead of launching particles uniformly from a circular perimeter, a von Mises distribution is used to simulate the preferential location of the source and lateral spread of released particles. For each α_p value, the location and concentration parameters of the von Mises distribution are modified.

For each of the scenarios a seed is placed at the center of a 512×512 matrix. The new particles are then released from a random position (according to a uniform or a von Mises distribution) on a distant circle, after which they move randomly in four directions on the square lattice (up, down, left, and right), six directions on the triangular lattice, or in an arbitrary direction for off-lattice simulations. Particles that reach the growing cluster stick with probability s [given by, e.g., Eq. (1)] or continue moving with probability $1-s$. Finally, the aggregation process is terminated when the cluster reached the size of 50 000 particles. Each growth condition is repeated 20 times to minimize variations due to random noise.

Another important aspect that depends on the system to simulate is the boundary condition. We initially set the release circle for particles to 150 and increase its radius to maintain a minimum distance between the circle and the cluster equal to $\Delta r = 100$ as the accumulated cluster grows. As opposed to the standard DLA model where particles are always launched from a distant circle (i.e., infinite launching distance), our choice of a small distance between the cluster to the launching circle was made to simulate elastic growth chambers comparable in size to the cluster itself, a situation frequently encountered in nature. For example, this models the growth of biostructures inside soft or growing membranes (such as agglomerates inside any cell or otoliths in the inner ear of fish and mammals). For permeable membranes, one can use the open boundary conditions, i.e., particles that reach the release circle during random motion are discarded. If unspecified otherwise, we used open boundary conditions in this work. However, we also performed some comparative calculations for a fully closed

system (i.e., when reaching the release circle, the random-walking particles bounce back inside).

III. MICROSCOPIC AGGREGATION AS A FUNCTION OF SURFACE TENSION

Figures 1 and 2 show clusters obtained in the scenario of the generalized DLA model [12] in a confined geometry. They are all isotropic or converge to an isotropic shape with the increase of the number of particles since the particles are released from a uniform random position and move according to a Brownian trajectory. The square symmetry observed for low values of α_p stems from the choice of the underlying square grid. Clusters obtained with a low α_p value are more compact,

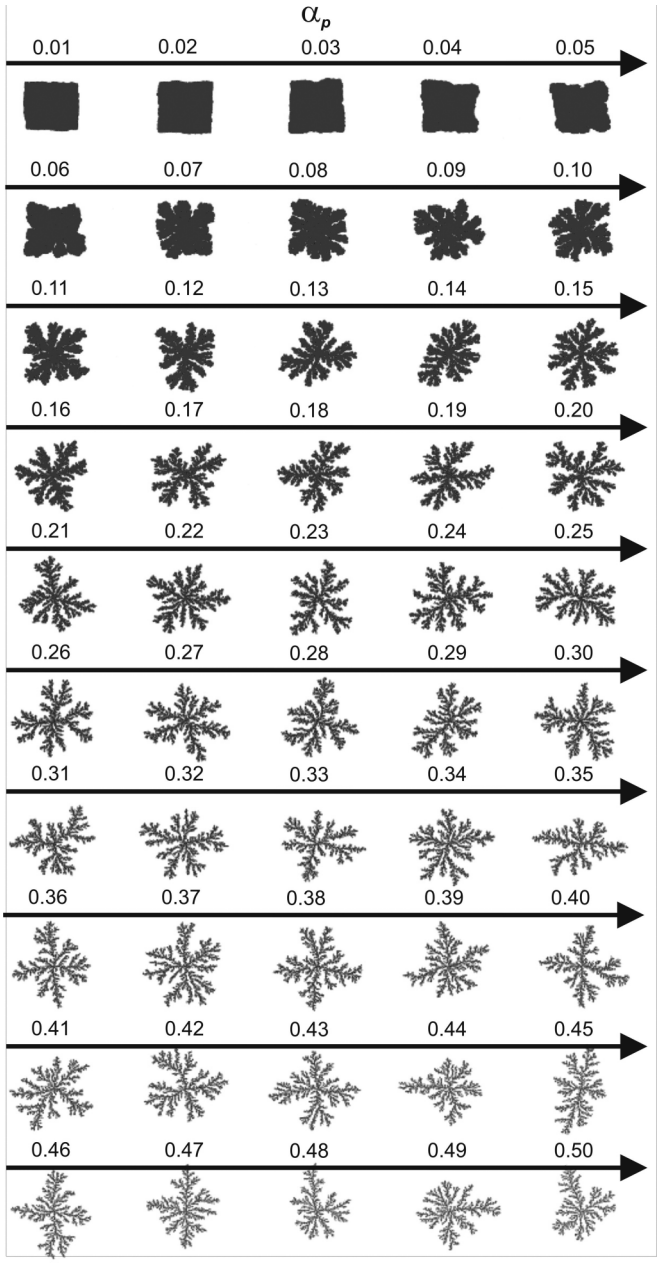

FIG. 1. Morphological diagram of clusters with 50 000 particles aggregated with different surface tension (α_p values).

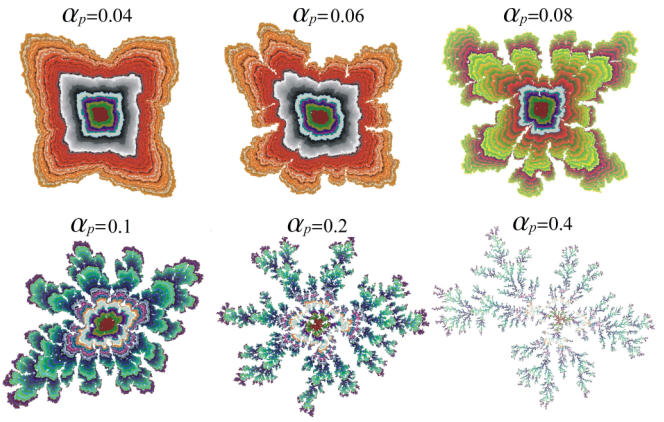

FIG. 2. (Color online) Exemplified clusters with 50 000 particles aggregated under different surface tension (α_p values). Here different colors reveal growth stages, each corresponding to 1000 aggregated particles.

resembling an Eden-like cluster [2], and the closer α_p gets to unity, the more standard (expected, DLA-like) the cluster becomes.

For DLA growth, the parameter α_p is analogous to the surface tension [3,12]. This analogy is often related to fluid-fluid interaction when the shape of the surface of a fluid depends of the properties of the surrounding fluid, such as viscous fingering [3]. The reference to the effect of surface tension on the form of aggregates was made by Thompson in 1917 to describe the form of aggregates of cells and tissues [18]. However, independently of the kind of phenomenon, the effect of surface tension results in minimizing the area and potential energy of the system. More precisely, surface tension reduces the surface in contact with the environment, as much as the present conditions and circumstances of growth will permit.

It can be seen in Fig. 1, and with more details in Fig. 2 for distinct growth stages (1000 particles at the time), that the lower α_p values yield stronger particle connections since the particle requires more neighbors to attach to the cluster. This results in a more dense cluster and a smoother reduced surface. Increasing α_p makes the border of the clusters more corrugated, with protrusions and cavities, increasing the interface with the environment. Hence, the way that particles connect with one another is an important characteristic that controls the shape of a structure in terms of surface roughness.

In nature, it is often true that growth of biological systems depends on the underlying lattice (e.g., protein network for otoliths). All observed structures in figures so far have quite common anisotropy, which may be reduced by using a different lattice for growth and/or different definitions of sticking probability (preferential growth directions). The latter was pointed out by Meakin [17] as important for the reduction of anisotropy. For this reason, we show in Fig. 3 the results obtained for square, triangular, and off-lattice simulations (the latter for either four or eight growth directions) for either open [Fig. 3(a)] or closed boundary conditions [Fig. 3(b)] and for varied surface tension. The observed effects of surface tension, already discussed in relation to Figs. 1 and 2, clearly

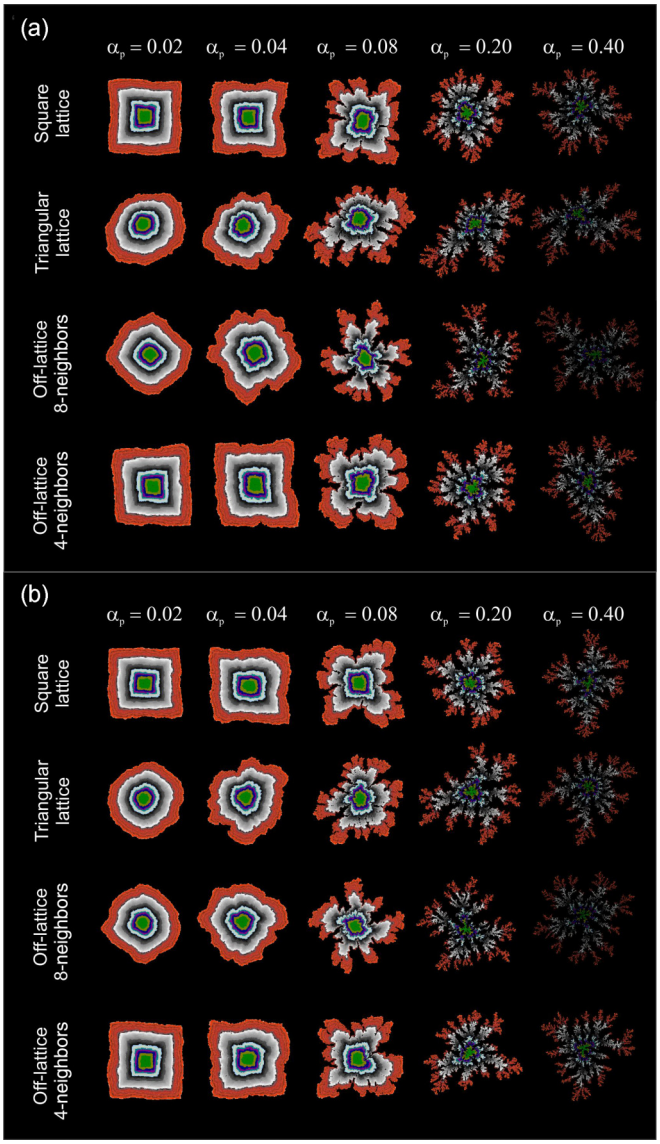

FIG. 3. (Color online) Comparison of clusters with 50 000 particles aggregated under different surface tension (α_p values) for different rules for the available directions in the random walk of particles and different allowed directions for growth, for either (a) open or (b) closed boundary conditions. Here different colors reveal growth stages, each corresponding to 1000 aggregated particles.

do not change if lower anisotropy of the underlying lattice is considered. A closed boundary condition is actually known to have no effect at all on the cluster structure, as previously observed by Havlin and Trus [19]. Imposed restrictions of the growth direction (i.e., the number of neighboring sites experienced by the incoming particle) appear to be more important for the shape plasticity of the aggregates than the restrictions in the available directions for the random walks. Rounder shapes are obtained using a triangular lattice or off-lattice DLA with 8-neighbors, while off-lattice DLA with 4-neighbors result in square shapes similar to the ones in simulations on a square lattice. Still, we conclude this section by reiterating that the reported physical effects of the surface tension do not depend on the chosen growth scenarios in Fig. 3.

IV. AGGREGATION AS A FUNCTION OF SURFACE TENSION AND DIRECTIONAL FLOW

In this section we address the scenario (ii) from Sec. II in terms of varied directional probabilities ρ_i and the sticking probability α_p (surface tension). In general, we observe a wide spectrum of shapes, where, as may be expected, the aggregates tend to grow more rapidly in the direction of the increased incoming flux, yielding anisotropic clusters.

In Fig. 4 we show the formed clusters under the influence of increased flow in one particular direction. Generally speaking, the higher the probability of a preferable direction, the less spread out the aggregate is, with suppressed branching. At the same time, the type of branches and surface of the cluster turn out to be very sensitive to the flux increase. More precisely, broader branches and a more compact surface are observed for higher fluxes, converging to a ballistic deposition aggregate [2]. This occurs because the growth probability in the interior of the cluster increases as the particles lose freedom of movement and go straight in some direction, such as in the case of am assembly of magnetic particles in magnetic field, particles in water current, or a gradient in environment density.

Note that the branch formation and their roughness are still more strongly related to α_p (the mechanism of particle aggregation) since branches are only observed for clusters with α_p higher than 0.1. This conclusion is general, as verified in our results for scenario (iii) (varied flux in two perpendicular directions), shown in Fig. 5. The only additional feature to note is that very asymmetric shapes can be obtained when the two varied probabilities are different from each other and different from those of other directions.

We point out here that the effects of flow in a particular direction can also be studied (more realistically, or at least with decreased influence of the underlying lattice) in the off-lattice model by taking a spread distribution of probabilities for particle motion centered around the preferential direction. To test our conclusions of this section on an off-lattice model, we used the von Mises distribution for motion probability (equivalent to a Gaussian distribution, but on a circle, as a function of angle x):

$$f(x,\mu,\kappa) = \frac{e^{\kappa\cos(x-\mu)}}{2\pi I_0(\kappa)}, \tag{3}$$

where $I_0(x)$ is the modified Bessel function, the preferential direction of flow is determined by the angle μ, and the spread of the distribution is controlled by the parameter κ (κ is a reciprocal measure of dispersion, so $1/\kappa$ is analogous to the variance of a normal distribution). We exemplified some characteristic results in Fig. 6, for off-lattice simulations with either 4- or 8-neighbors, only to conclude that our findings of the present section, based on a simplified model, still hold. In the von Mises implementation of the preferential flow, the obtained structures are elongated in the direction prescribed by angle μ and lateral extension of the cluster as well as its branching are governed by κ (increasing $1/\kappa$ decreases the probability of motion in the preferential direction and increases the probability of motion laterally to the preferential direction). In Fig. 6 we deliberately show results for very small α_p (=0.02), where compact structures are expected and all observed peripheral branching is due to the flow

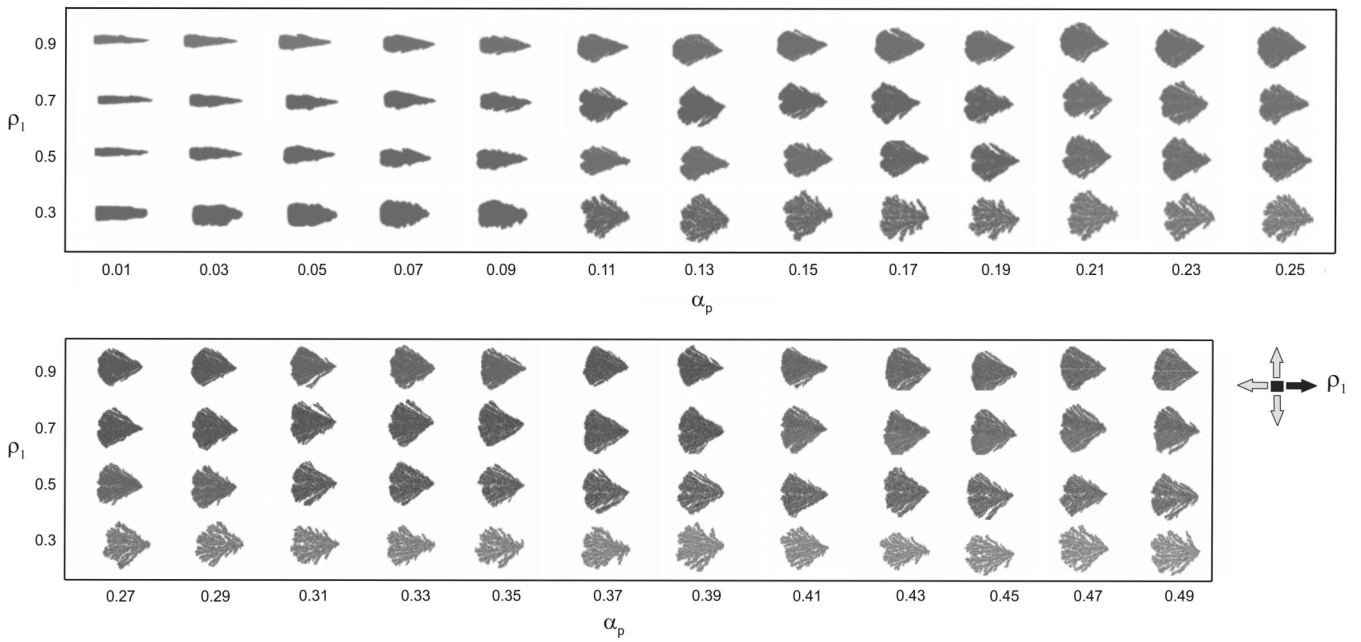

FIG. 4. Morphological diagram of clusters with 50 000 particles aggregated for different surface tension (α_p, on the x axis) and flow (ρ_1, as depicted in the inset, varied on the y axis).

(as emphasized before, larger α_p always enhances branching effects).

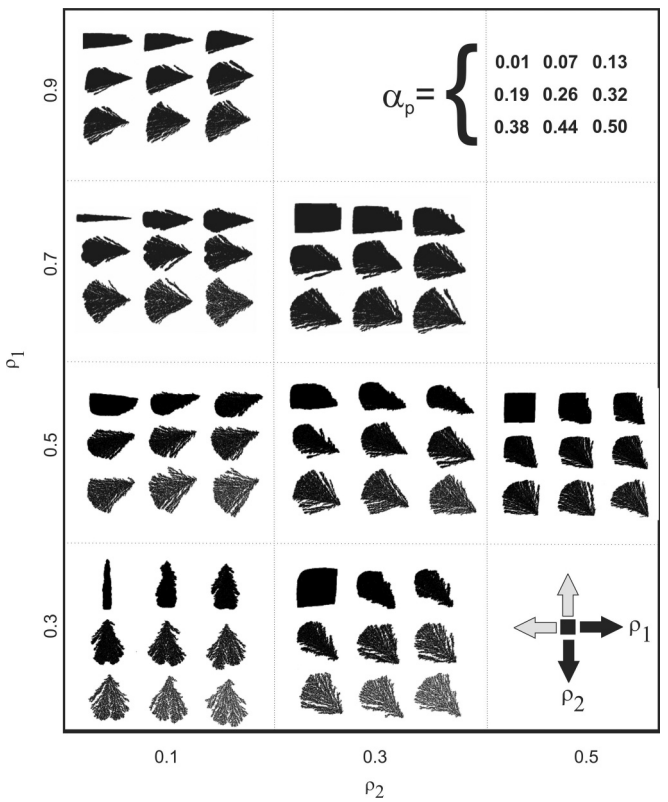

FIG. 5. Morphological diagram of clusters with 50 000 particles aggregated for varied flow probabilities ρ_1 (left to right) and ρ_2 (top to bottom) and probabilities for the two remaining directions $\rho = (1 - \rho_1 - \rho_2)/2$. In each image, a sequence of clusters is shown for varied sticking probability $\alpha_p = 0.01$–0.5, as shown in the dedicated inset.

V. AGGREGATION AS A FUNCTION OF SURFACE TENSION AND LOCALIZED PARTICLE SOURCE

In the previous scenarios the particles were released from a uniformly chosen random position on the circular perimeter that envelopes the cluster. In this section we discuss cluster growth when predefined localization of the particle source is used, e.g., based on a von Mises distribution (with $\mu = 3\pi/2$

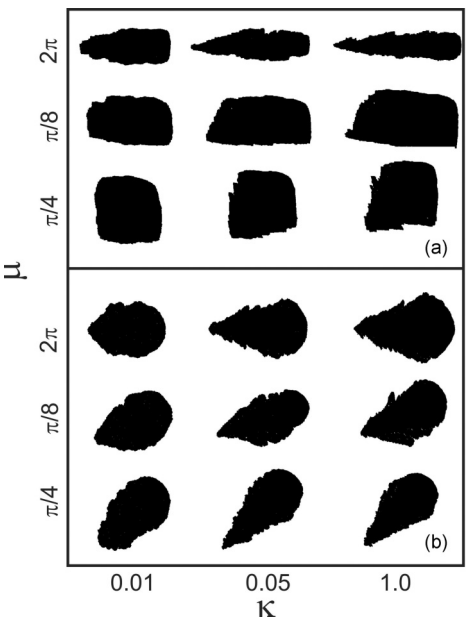

FIG. 6. Diagram of clusters with 50 000 particles aggregated for varied preferential direction of flow (angle μ) and dispersion of the von Mises distribution for motion probabilities $1/\kappa$, sticking probability $\alpha_p = 0.02$, and off-lattice model with (a) 4-neighbors or (b) 8-neighbors.

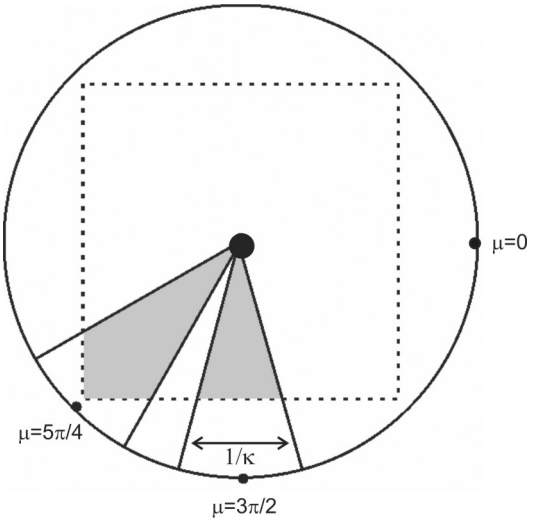

FIG. 7. Schematic representation of the location parameter μ for the source of incoming particles and the importance of its choice compared to the underlying (in this case square) grid in the simulation. Here κ is the concentration parameter of the von Mises distribution used to choose the site on the perimeter from which the particle is released.

or $5\pi/4$, as shown in Fig. 7). In other words, the source point was put at the perimeter, with location determined by the angle μ, and then the von Mises distribution was applied so that incoming particles were generated around the source point with a spread controlled by the parameter κ.

The taken choice of source locations is significant for the visual appearance of the final shape of the clusters, trapezoidal for $\mu = 3\pi/2$ (270°) and leaflike for $\mu = 5\pi/4$ (225°) (see Fig. 8), resulting from the fact that the square grid was used in the simulations. More precisely, for low α_p values, if a random source of particles is used the resultant shape is a

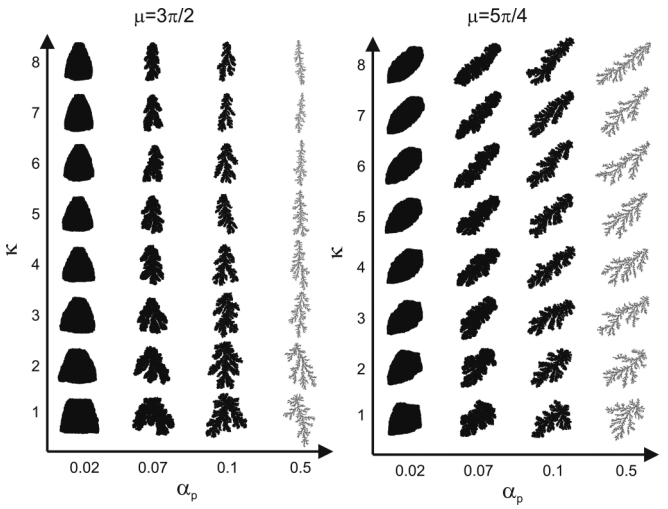

FIG. 8. Morphological diagram of clusters with 50 000 particles aggregated under different surface tension α_p and for different concentration of released particles (parameter κ), considering two locations of the particle source (i.e., angle μ, marking the maximum of the distribution of the released particles on a distant circle).

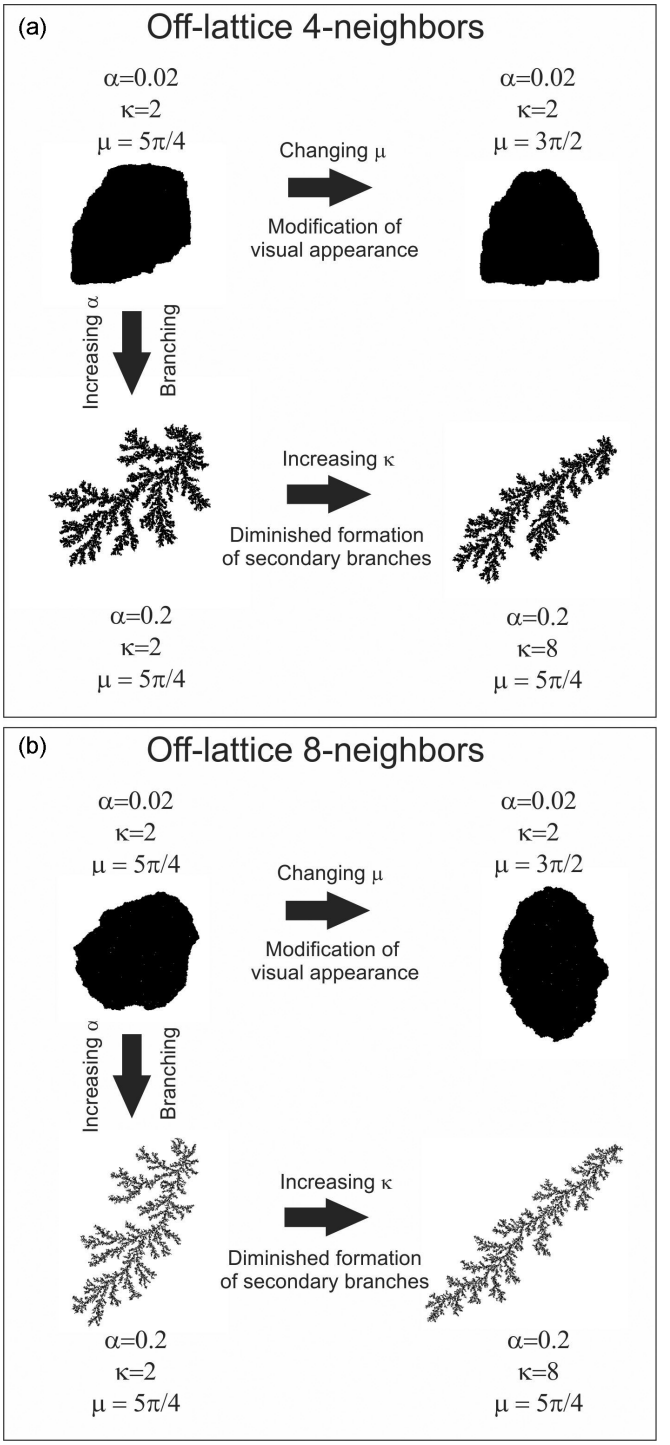

FIG. 9. Summarizing figure for Sec. V, showing the influence of parameters of the nonuniform distribution of released particles and the surface tension on the obtained aggregates with 50 000 particles for the off-lattice DLA model used with either (a) 4-neighbors or (b) 8-neighbors.

square (Fig. 1); in the case of $\mu = 3\pi/2$, the frontal side to the source is flat and the cluster narrows away from the source shape; finally, for $\mu = 5\pi/4$ the vertex of the square is obtained frontal to the source, decaying into a point apex away from the source (see Fig. 8). The schematic representation in Fig. 9

reinforces the strong relationship between the source location and the underlying lattice for the growth, independently of the restriction in the allowed directions for the random walks. Namely, in Fig. 9 off-lattice motion of particles was adopted (i.e., a continuous random walk of particles), but a strong difference in anisotropy was observed depending on the chosen geometry for cluster growth (i.e., the number of neighbors in the model).

However, regardless of the chosen model or lattice, in the case of higher surface tension, more developed lateral and secondary branches are observed (see Fig. 8 for square lattice DLA), all widening for decreased κ values (i.e., spread out and a lower concentration of incoming particles). This is confirmed for an off-lattice DLA (Fig. 9), independently of the number of neighboring sites experienced by the incoming particle.

This exercise is important for two reasons. First, it is frequently the case in nature that the source of particles to assemble is localized and the effects of such localization should be understood. Naively, one often identifies the preferential unidirectional flow with a localized source of particles, while their differences are very clear from Figs. 2 and 8, respectively. For example, for a weak surface tension (large α_p), the large flow leads to large fanning out of the dendritic branches of the cluster, whereas large localization and concentration of incoming particles lead to a practically linear stem with weak and roughly uniform lateral branching along it. The second important aspect of this section is to pinpoint the influence of the location of the source on the anisotropy of the aggregate due to the geometry of the underlying matrix for the aggregation.

VI. SIMILARITIES TO NATURAL STRUCTURES

The behavior of aggregation growth shown in Sec. III is typically observed during the biomineralization process, especially during the assembly of crystalline polymorphic structures composed of calcium carbonate: calcite, aragonite, and vaterite. The growth of these crystalline polymorphs can be both environmentally and genetically regulated. More precisely, modifications of the environmental [20] or of genetic conditions [4] can change the way that molecules aggregate and consequently also change the morphology of the resulting structure.

Such modifications are readily observed in biominerals such as otoliths, where, e.g., vaterinic otoliths are frequently abnormal [21], bigger, and less dense [22]. For example, experiments demonstrate that the zebrafish otoliths present a rough surface [a star-shaped otolith; see Fig. 10(c)] rather than the regular smooth appearance [a wild-type otolith; see Fig. 10(a)] when the gene starmaker activity is reduced [4]. It is implied that modification of this gene affects the level of protein formation and hence causes changes in the structure of the protein matrix, in the crystalline polymorph, and consequently in the formation of the calcium carbonate crystal. Comparing Fig. 1 with Fig. 10, one could see that the change of the otolith shape by the reduction of starmaker activity demonstrates behavior strongly resembling our simulated structures when α_p is increased (decreasing surface tension).

As another example we show the crystal in Fig. 11 that is very similar in appearance to the cluster obtained for $\alpha_p = 0.08$ in Fig. 2. This crystal structure was obtained

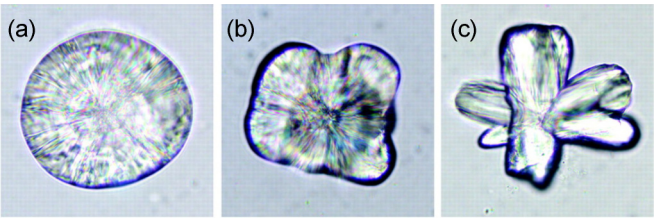

FIG. 10. (Color online) Otoliths of zebrafish after gradual reduction of activity of the starmaker gene, from Söllner *et al.* [4]: (a) wild-type otolith, (b) slightly irregular otolith obtained after intermediate reduction, and (c) star-shaped otolith obtained after strong reduction.

after an experimental process of emulated osseointegration on titanium implant surface, by submersion in an artificial corporal fluid. In this experiment it was observed that the agglomeration pattern is governed by the topology (roughness) of the implant surface. It is plausible that the surface roughness of the substrate projects itself onto the energetically favorable shape of the growing crystal, i.e., a desirable surface tension for the agglomerate, so that our DLA cluster for $\alpha_p = 0.08$ nicely matches the resulting structure.

Our third example outside the usual applications of DLA concerns stony corals. In Ref. [5] Merks *et al.* concluded that branch formation in stony corals is spontaneous in their Laplacian-based growth model and that compactness of the corals depends on the ratio of the rates of growth and nutrient transport. In a subsequent work [23] the same authors stated that the spacing of polyps influences the thickness of branches and the overall compactness. The results obtained by the present generalized DLA model indicate that branch formation in the clusters depends primarily on the surface tension α_p and the thickness of branches and the overall compactness depend on both surface tension and flow.

In Fig. 12 we show some available data from the literature, where stony corals that grew in a sheltered site were found to have a more open branched structure than those species that

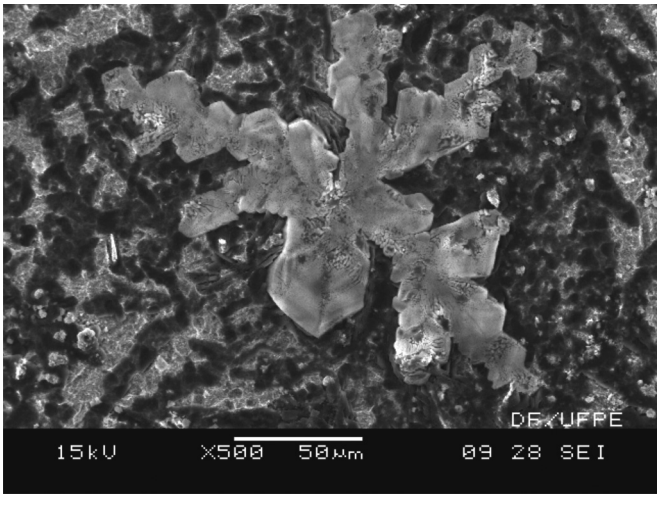

FIG. 11. Electron microscopy image of a crystal formation on an implant surface treated with calcium phosphate and acid.

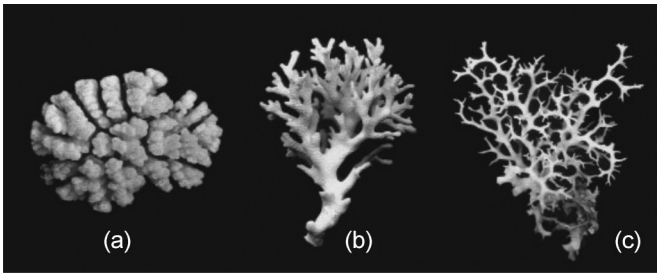

FIG. 12. Growth forms of the stony coral *Pocillopora damicornis* (from Kaandorp *et al.* [7]; original from Veron and Pichon [24]). The forms originate from (a) an exposed site, (b) a semiprotected site, and (c) a site sheltered from water movement.

are collected from an exposed site [5]. In Sec. V we showed that wider shapes and more developed secondary branches are observed for a broader spread of released particles [lower κ of the von Mises distribution (see Fig. 8)] and the cluster becomes more compact as the surface tension is changed (α_p is made lower). The corals in a sheltered site arguably have access to fewer (and widely distributed) resources for growth, as well as to a low concentration of nutrients. The former corresponds to low κ in our von Mises distribution, whereas the latter causes the surface of the coral to enlarge for efficient feeding, i.e., surface tension lowers, i.e., larger α_p is envisaged for our model. It is therefore of no surprise that the observed changes in the structure of the cluster in Fig. 8 going diagonally from high κ and low α_p to low κ and high α_p nicely correspond to the changes shown in Figs. 12(a)–12(c).

Quantification of similarity

In this article we have dealt primarily with the observable physical effects of several ingredients in the DLA model on the obtained aggregates. It is, however, frequently the case that obtained morphologies need to be further analyzed, classified, or their particular features linked to the known ongoing processes in nature during growth of a particular simulated system. In this section we propose the use of the contour fluctuations of the aggregates for the comparison between the details of the DLA aggregates and the simulated system, based on which DLA model can be further improved. In nature, fluctuations in the boundary of a natural structure during growth are a response to surface interaction and the internal mechanisms of the growth process and these fluctuations can be easily obtained from just images of any natural structure.

We analyzed these fluctuations using the recently proposed traveling observer contour decomposition [25]. The idea behind this technique is to map the contour of the observed structure onto a time series of radial distances from the actual contour, as seen by a virtual observer traveling along the zeroth harmonic (best fit circle), at constant angular speed. This sequence of distances (considered here as a time series) captures the fluctuations in a sequential (directional) manner.

More precisely, the x and y coordinates of the cluster contour pixels were used to determine the radius of each contour point with respect to the center of mass, as well as the average radius of the structure a_0 (zeroth harmonic) used to normalize the individual contour pixel radii. Thus, for each aggregate (obtained for a given set of input parameters) a series of normalized radii from $-\pi$ to π was obtained as $r_c(\varphi) = \sqrt{x^2 + y^2}/a_0$. Therefore r_c, at a certain angle φ, is less than one if the contour point lies inside the circle and it is greater than unity if the point lies outside the circle.

One interesting possibility to extract information from the contour fluctuations is to deploy a multifractal analysis of the above time series (see, e.g., [25] and references therein). Although that method may reveal a plethora of information, the link between the observed physical phenomena and the multifractal parameters is often nontrivial to make. Therefore, in this article we opt for an alternative method. For the purpose of quantifying the similarity among the real and the simulated shapes we propose the following procedure.

To make the comparison of N shapes (some of which may be the result of simulation, while others may represent real structures), we first perform a mapping of all the considered shapes to the corresponding normalized time series r_{ij} ($i = 1,\ldots,N$; $j = 1,\ldots,n_i$), where n_i is the number of contour pixels of the ith shape, consecutively distributed between $\varphi = -\pi$ and π. Next the maximum number of observed shape pixels $n = \max(n_i)\,(i = 1,\ldots,N)$ is found and for the purpose of mutual comparison all the series with $n_i < n$ are (linearly) interpolated to produce coincident series r^*_{ij} ($i = 1,\ldots,N$; $j = 1,\ldots,n$). An example of such a normalized aligned sequence for two otoliths and a simulated aggregate is shown in Fig. 13.

The distance between any two series $\ell = 1,\ldots,N$ and $m = 1,\ldots,N$ can now be defined as

$$d^*_{\ell-m} = \sqrt{\frac{1}{n}\sum_{j=1}^{n}(r^*_{\ell j} - r_{mj})^2}. \tag{4}$$

This measure of the difference between series is, however, dependent on the rotation and reflection on an (arbitrary) axis passing through the shape's center of mass, so for each pair of shapes we also perform reflection on the axis $y = 0$ of one of the shapes of the considered pair and rotation at

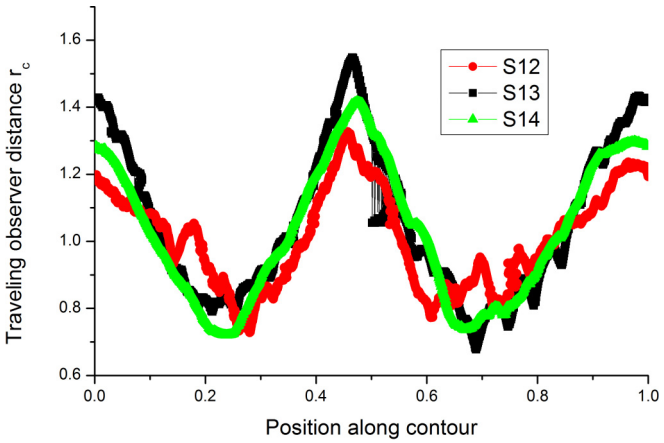

FIG. 13. (Color online) Example of three series generated by the traveling observer contour decomposition (corresponding to shapes 12–14 in Fig. 14) after interpolation, reflection, and rotation. Pairwise distances among series are $d_{12\text{–}13} = 0.130$, $d_{13\text{–}14} = 0.070$, and $d_{12\text{–}14} = 0.108$.

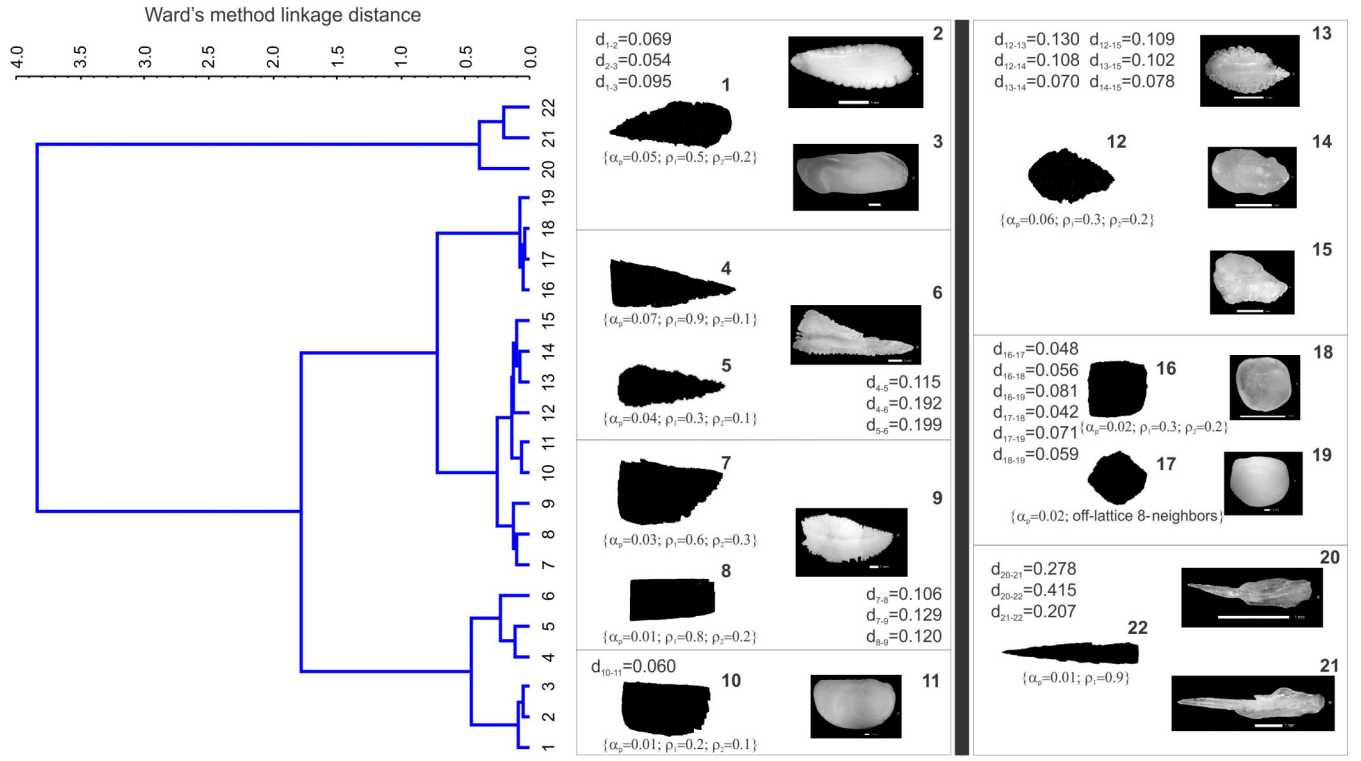

FIG. 14. (Color online) Similarity analysis of simulated aggregates obtained in this paper and experimental images of real otoliths. The tree classification (on the left-hand side) was carried out based on Ward's method [26]. Images grouped together by cluster analysis (thus shown to be similar) are displayed on the right-hand side, where pairwise distances among structures are also indicated. The parameter sets used to generate the artificial aggregates are shown in curly brackets below each image.

$j = 1, \ldots, n$ possible angles to find the minimum distance $d_{\ell-m} \equiv \min(d^*_{\ell-m})$ for all the reflection and rotation options. Finally, the obtained minimal d is considered as a similarity measure between two series.

By considering all the pairs of the N compared shapes, a distance matrix is produced, which can then be used within any conventional amalgamation (linkage) schedule, such as Ward's method [26], to perform a hierarchical (tree) classification of the considered shapes. We demonstrate this in Fig. 14 using experimental data of several real fish otoliths and artificial aggregates generated in scenarios (i)–(iii) of the current work. It is clearly shown in Fig. 14 that the currently proposed procedure yields a rather convincing hierarchical classification of real and simulated aggregates, which may serve as a starting point in the quest for the best set of model parameters, pertinent for describing a given real physical aggregate. It also follows from Fig. 14 that flux may be one of the most important factors that control the overall shape of otoliths. Shape anisotropy of fish otoliths caused by particle flux was also observed experimentally by Wu *et al.* [27]. They found that the pronounced anisotropy of otoliths (which is rather common) may be attributed to different growth probabilities on sites exposed to the flux of incoming particles, due to their confinement in the inner ear of the fish. This finding is corroborated by the simulations performed in the present work. Furthermore, this suggests that generalizations of the DLA model presented in this paper make possible a rather realistic modeling of the fish otolith growth, even though the model does not explicitly contain microscopic, genetic, or environmental mechanisms that control the otolith morphogenesis.

In a more general context of growth of biomineral structures, such as growth and branching of stony corals, judging from the diversity of shapes produced by the generalized DLA model presented in this work, one may again expect a close match between real shapes and the shapes obtained through simulated aggregation for a suitable choice of model parameters. On the other hand, the precise relationship between the best model parameters (that yield the minimal distance between the real and simulated shapes) and the actual microscopic mechanisms responsible for the observed growth phenomenon remains to be elucidated for each particularly considered aggregation phenomenon in nature.

VII. SUMMARY

In this paper we analyzed the combined effect of three added ingredients to a diffusion-limited-aggregation model, which seem to be quite intrinsic to many aggregation growth processes found in nature. The surface tension is a property that is very much controlled by environmental conditions, substrate, and desired functions of the growing structure. The particle flow and particle source are also commonly encountered conditions in nature, as the source is frequently localized and the flow (or external field, gravity, etc.) is characteristic of many systems. The preferential flow direction and source location of incoming particles can significantly effect the shape, primary and secondary branching, and

thickening of the aggregate, while the surface tension controls the roughness of the border or surface. Our systematic analysis of aggregation in a loosely confined geometry showed that when combined, these ingredients generate a wide range of shapes, making their competing effects fundamental for modeling growth phenomena of structures in confined or sheltered spaces and/or in the presence of external fields, such as rocks, crystals, biominerals, and corals.

ACKNOWLEDGMENTS

This work was supported by CNPq, Brazil (Projects No. 201506/2011-4, No. 303251/2010-7, and No. 306719/2012-6). M.V.M. acknowledges support from Flemish Science Foundation (FWO-Vlaanderen) and CAPES PVE action No. BEX1392/11-5. The crystal structure appearing in Fig. 11 was provided courtesy of L. dos Santos, UFPE, Brazil.

[1] T. Vicsek, *Fractal Growth Phenomena* (World Scientific, Singapore, 1989).
[2] A.-L. Barabási and H. E. Stanley, *Fractal Concepts in Surface Growth* (Cambridge University Press, Cambridge, 1995).
[3] P. Meakin, F. Family, and T. Vicsek, J. Colloid Interface Sci. **117**, 394 (1987).
[4] C. Söllner, M. Burghammer, E. Busch-Nentwich, J. Berger, H. Schwarz, C. Riekel, and T. Nicolson, Science **302**, 282 (2003).
[5] R. Merks, A. Hoekstra, J. Kaandorp, and P. Sloot, J. Theor. Biol. **224**, 153 (2003).
[6] T. A. Witten and L. M. Sander, Phys. Rev. Lett. **47**, 1400 (1981).
[7] J. A. Kaandorp, C. P. Lowe, D. Frenkel, and P. M. A. Sloot, Phys. Rev. Lett. **77**, 2328 (1996).
[8] W. G. Hanan and D. M. Heffernan, Phys. Rev. E **85**, 021407 (2012).
[9] P. Meakin and J. M. Deutch, J. Chem. Phys **80**, 2115 (1984).
[10] R. F. Voss, Phys. Rev. B **30**, 334 (1984).
[11] T. Vicsek, Phys. Rev. A **32**, 3084 (1985).
[12] M. Batchelor and B. Henry, Phys. A **187**, 551 (1992).
[13] P. Meakin, Phys. Rev. B **28**, 5221 (1983).
[14] T. Nagatani and F. Sagués, Phys. Rev. A **43**, 2970 (1991).
[15] L. López-Tomàs, J. Claret, F. Mas, and F. Sagués, Phys. Rev. B **46**, 11495 (1992).
[16] M. Batchelor and B. Henry, Phys. A **193**, 553 (1992).
[17] P. Meakin, Phys. Rev. A **33**, 3371 (1986).
[18] D. W. Thompson, *On Growth and Form* (Dover, New York, 1992).
[19] S. Havlin and B. L. Trus, J. Phys. A: Math. Gen. **21**, L731 (1986).
[20] S. B. Mukkamala, C. E. Anson, and A. K. Powell, J. Inorg. Biochem. **100**, 1128 (2006).
[21] R. W. Gauldie, S. K. Sharma, and E. Volk, Comp. Biochem. Physiol. **118A**, 753 (1997).
[22] D. S. Oxman, R. Barnett-Johnson, M. E. Smith, D. L. M. Allison Coffin, R. Josephson, and A. N. Popper, Can. J. Fish. Aquat. Sci. **64**, 1469 (2007).
[23] R. M. H. Merks, A. G. Hoekstra, J. A. Kaandorp, and P. M. A. Sloot, J. Theor. Biol. **228**, 559 (2004).
[24] J. E. N. Veron and M. Pichon, *Scleractinia of Eastern Australia Part 1*, Australian Institute of Marine Science Monograph Series Vol. 1 (Australian Government Publishing Service, Canberra, 1976).
[25] P. Duarte-Neto, B. Stošić, T. Stošić, R. Lessa, M. Milošević, and H. E. Stanley (unpublished).
[26] J. H. Ward, J. Am. Stat. Assoc. **58**, 236 (1963).
[27] D. Wu, J. B. Freund, S. E. Fraser, and J. Vermot, Dev. Cell **20**, 271 (2011).